IJE TRANSACTIONS A: Basics Vol. 27, No. 10, (October 2014) 1511-1518

International Journal of Engineering

Journal Homepage: www.ije.ir

TECHNICAL NOTE

# Studying Performance of Dubinin-astakhov and Dubinin-raduchkevic Equations to Evaluate Nanopore Volume and Pore Size of MCM-41 Particles

N. Saeidi, M. Parvini*, M. R. Sarsabili

*School of Chemical, Gas and Petroleum Engineering, Semnan University, Semnan, Iran*

*PAPER INFO*

*Paper history:*
Received 15 February 2014
Received inrevised form 18 June 2014
Accepted 26 June 2014

*Keywords*:
Nitrogen Isotherm Data,
MCM-41
Dubinin-astakhov and Dubinin-Raduchkevic Equations
Nanopore (Mesopore) Volume
Pore Size

*ABSTRACT*

MCM-41 particles were synthesized using inorganic raw materials and Cetyltrimethylammonium bromide (CTAB). The textural properties and structure of MCM-41 particles were characterized by X-ray diffraction (XRD), scanning electron microscope (SEM), transmission electron microscope (TEM) and $N_2$ adsorption-desorption methods. To study performance of Dubinin-Astakhov and Dubinin-Raduchkevic isotherm models in evaluating mesopore volume and pore size of MCM-41 samples, the mesopore volume and pore size of several MCM-41 samples were calculated by means of two mentioned isotherm models and by utilizing $N_2$ adsorption isotherms and XRD data. The obtained results were compared with the mesopore volume and pore size calculated by other methods. The results showed that the calculated mesopore volume and pore size on the samples with the fraction of mesopore volume > 0.9 had not good consistency with XRD data and the results obtained by other methods. However, the calculated mesopore volume and pore size on the samples with the fraction of mesopore volume ≤ 0.9 were in good agreement with XRD data and other advanced simulation techniques.
.

*doi: 10.5829/idosi.ije.2014.27.10a.04*

## NOMENCLATURE

| | | | |
|---|---|---|---|
| $w$ | Represents the volume of adsorbate filling the micropores ($cm^3/g$) | $\lambda$ | wavelength of Cu Ka radiation |
| $V$ | Volume of pores | $m$ | mass of an electron |
| $S$ | Surface area | $E_0$ | Characteristic energy of adsorption |
| $a_m$ | Molecular area of nitrogen | $P_0$ | Saturation vapor pressure |
| $V_{total}$ | Total pore volume | $R$ | Universal gas constant |
| $D_{XRD}$ | Mesopore diameter for MCM-41 | $d_0$ | Mean diameter of the adsorbate molecule |
| $V_p$ | Mesopore volume | $\Delta G$ | Differential Gibbs energy of adsorption |
| $d_{100}$ | XRD interplanar spacing | $A$ | Differential molar work of adsorption |
| $T$ | Temperature | $n$ | Equation parameter |
| $P/P_0$ | Relative pressure | **Greek Symbols** | |
| $w_0$ | Maximum volume of adsorbent per adsorbed mass ($cm^3/g$) | $\rho$ | Density of the silica |
| $\theta$ | situation of the first low-angle peak | $\alpha_0$ | Lattice parameter |

*Corresponding Author's Email: m.parvini@sun.semnan.ac.ir (M. Parvini )

Please cite this article as: N. Saeidi, M. Parvini, M. R. Sarsabili, Studying Performance of Dubinin-astakhov and Dubinin-raduchkevic Equations to Evaluate Nanopore Volume and Pore Size of MCM-41 Particles, International Journal of Engineering (IJE), TRANSACTIONS A: Basics Vol. 27, No. 10, (October 2014) 1511-1518

## 1. INTRODUCTION

MCM-41 was introduced in 1992. Thereafter, there have been five major courses for studying about this material. These entail characterization, mechanism of formation, synthesis of new materials based upon MCM-41, control of textural characterizations and various industrial applications [1, 2]. MCM-41 material is very interesting for many of researchers because of its structural properties (mesopore structure) provides the pore size needed for different applications i.e., catalysts for various fine chemical syntheses and adsorbing a relatively wide range of size of molecules of gas and liquid [2, 3]. Therefore, it is very vital to control and examine morphology of MCM-41. The textural properties of MCM-41 are very often determined by gas ($N_2$) adsorption isotherm and XRD data [2, 4-8].

The empirical form of an adsorption isotherm was identified in 1926 by Freundlich [9] and was later deduced theoretically from the Langmuir equation [10] extended to heterogeneous surfaces considered to be a composite surface, mixed of many homogeneous patches [11]. By confirming the Langmuir mechanism, but considering a number of assumptions, the Brunauer–Emmet–Teller (BET) equation was derived for multilayer adsorption [12]. It is clear that together with the concept of multilayer adsorption (leading to the BET equation) the theory of volume filling of micropores is one of the most motivation concepts taking up the principal position in adsorption science [13].Based on the Weibull distribution of adsorption potential, the introdused equation by M. M. Dubinin [13] was considered to be a semi-empirical one. The basic relations are the Dubinin-Astakhov (DA) and Dubinin-Raduchkevic (DR) equations [14, 15]. The DA and DR equations were very often applied for evaluating micropore volume of porous material such as activated carbon. In such works, the mesopore volume of sample was obtained by subtracting the total pore volume and the micropore volume of a sample [16-18]. The mesopore volume of MCM-41 was frequently calculated by Barrett–Joyner–Halenda (BJH) method [4-6, 19]. It is worthy to say using DA and DR equations to calculate mesopore volume and pore size of MCM-41 samples is swift and neat, and also the respective procedure to reach the desired results by these two models is easier and faster than that of BJH method. However, there is a questionable matter about accuracy in such functions. To our knowledge, performance of using DA and DR equations to assess mesopore volume and pore size of MCM-41particles has not been examined yet.

In the present study, the MCM-41 particles were synthesized. XRD pattern, $N_2$ adsorption-desorption isotherm, TEM and SEM were applied to examine the crystal structure, morphology and porosity of the synthesized MCM-41. Then, the mesopore volume and pore size of several MCM-41 samples were calculated using Dubinin-Astakhov and Dubinin-Raduchkevic equations. To this purpose, nitrogen adsorption isotherms and XRD data were used. Finally, the obtained results were compared with the mesopore volume and pore size calculated using other methods.

## 2. EXPERIMENTAL

**2. 1. Material** Cetyltrimethylammonium bromide (CTAB), tetraethylorthosilicate (TEOS), aqueous ammonia (25% w/w) and ethanol (96%) all were purchased from Merck. Deionized water was used as a main solvent. All chemicals were used as purchased and no further purification was performed.

**2. 2. Synthesis of MCM-41 Particles** The mesoporous silica was synthesized following the literature procedure reported by Grun et al.[20] with several alterations. In this synthesis, the source of silicon was tetraethylorthosilicate (TEOS) and the structure-directing agent was Cetyltrimethylammonium bromide (CTAB). The surfactant (15.1 g) was dissolved in deionized water (100.02 g) in ambient condition. Then, the ammonia solution (37.38 ml) was added into the solution. After about 10 min stirring at 200 rpm, a clear solution was obtained. Afterward, Ethanol (151.89 ml) was added in to the solution. After about 20 min, TEOS (4 ml) was slowly added into the clear solution. The resulting milky solution was stirred at 200 rpm for 2 hours. Finally, the white precipitate was filtered and washed with desired amount of deionized water and then dried at 100 °C for 48 hours. The silicate powder was calcined in air at 550 °C for 6 hours with 1 °C $min^{-1}$ of heating rate to remove the CTAB.

**2. 3. Characterization** The XRD patterns were obtained by using a PW1840 diffractometer employing Cu Kα radiation ($\lambda$ = 1.54056 Å), $\theta$– 2$\theta$ geometry and a scintillation detector. Each diffraction pattern was recorded at a step of 0.04° and 0.5 second per step. The measurements were made at ambient condition. A morphological characterization of the MCM-41 was carried out with a scanning electron microscope (MIRA//TESCAN). The transmission electron micrographs (TEM) were attained on a Philips (CM120) transmission electron microscope device with a field emission gun at an acceleration voltage of 120 kV. The nitrogen adsorption and desorption isotherms for the MCM-41 sample was measured at − 196 °C on a Belsorp 18 (BEL Japan, Ltd.). The sample was heated at 200 °C for 2 hours and degassed overnight. The specific surface area was determined by the Brunauer–Emmet–Teller (BET) method [11] using $a_m$ ($N_2$ = 16.2

Å$^2$), where, $a_m$, is the molecular area of nitrogen at −196 ˚C. The BET formula is valid over a range of $N_2$ relative partial pressure $P/P_0$ varying from 0.01 to 0.30 [12, 16]. Accordingly, the BET surface area of the MCM-41 was calculated on the mentioned range of relative partial pressure. The mesopore volume and the pore size of MCM-41 were determined based on BJH method [20].The mean pore diameter was also calculated using $D = 4V/S$[21], where $V$ is the volume of pores, and $S$ being the surface area. The total pore volume, $V_{total}$, was obtained using the adsorbed nitrogen at a relative pressure $P/P_0$ of approximately 0.99.

## 3. THEORETICAL APPROACH

The isotherm models, Dubinin-Astakhov and Dubinin-Raduchkevic equations, are given, respectively, in the following forms [14, 15]:

$$w = w_0 \exp\left[-\left(\frac{A}{bE_0}\right)^n\right] \quad (1)$$

$$w = w_0 \exp\left[-B\left(\frac{T}{b}\right)^2 \log^2\left(\frac{P_0}{P}\right)\right] \quad (2)$$

In Equatios (1) and (2), $w$ represents the volume of adsorbate filling the micropores, in the unit mass of adsorbent (cm$^3$/g), at temperature $T$ and relative pressure $P/P_0$, $w_0$ is the maximum volume of adsorbent per adsorbed mass, the micropore volume (cm$^3$/g), $B$ is a parameter characterizing the microporous structure, $\beta$ is the affinity coefficient of the characteristic curves, $E_0$ is the characteristic energy of adsorption, $n$ is an equation parameter and $A$ is the differential molar work of adsorption i.e., the differential Gibbs energy of adsorption, $\Delta G$, defined by Equation (3) as follows [14]:

$$A = -\Delta G = RT \ln\left(\frac{P_0}{P}\right) \quad (3)$$

It must be noted that the DA equation is valid at the micropore filling mechanism, over a range of $N_2$ relative partial pressure $P/P_0$ varying from 1E-7 to 0.02, and the DR equation is valid at both micropore filling and sub-monolayer formation mechanisms, over a range of $N_2$ relative partial pressure $P/P_0$varying from 1E-7 to 0.02 and 0.01 to 0.1, respectively.

The mesopore diameter for MCM-41, $D_{XRD}$, can be calculated from the mesopore volume, $V_p$, and the lattice parameter, $\alpha_0$, of the mesopore lattice, concluded from XRD data, according to the Equation (4) [22, 23]:

$$D_{XRD} = C a_0 \left(\frac{r V_P}{1 + r V_P}\right) \quad (4)$$

where $C = \sqrt{\frac{2\sqrt{3}}{p}} \approx 1.05$ and $\rho$ is density of the silica. The lattice parameter, $\alpha_0$,is expressed by Equation (5) [22, 23]:

$$a_0 = \frac{2d_{100}}{\sqrt{3}} \quad (5)$$

where, $d_{100}$ is the XRD interplanar spacing calculating by Equation (6) [22, 23]:

$$d_{100} = \frac{l}{2\sin q} \quad (6)$$

where, $\lambda$ is a wavelength of Cu Ka radiation and $\theta$ is the situation of the first low-angle peak /°.

In Equation (4), the mesopore volume, $V_p$, can be calculated using various methods including BJH method. The mesopore volume can also be computed by subtracting the total pore volume of sample, $V_{total}$, from the micropore volume of sample obtained by both DA and DR models, $w_0$. Therefore, Equation (4) is subsequently rewritten as follows [6]:

$$D = C a_0 \left(\frac{r (V_{total} - w_0)}{1 + r (V_{total} - w_0)}\right) \quad (7)$$

Where $C$, $w_0$, $\alpha_0$ and $\rho$ parameters are the same as the parameters introduced in Equations (4), (1), (5) and (4), respectively. Also, $V_{total}$ denotes total pore volume of the sample.

## 4. RESULT AND DISCUSSION

### 4. 1. Characterisation of MCM-41 Particles

XRD experiment was performed to determine the specific structure of the obtained sample. The XRD result was illustrated in Figure 1. It can be deduced that the structure of MCM-41 particles is arranged very well and has the same patterns as the MCM-41 synthesized by other authors [2, 24-27]. The major characterization of MCM-41 can be studied from presence of three distinctive reflections at $2\theta$ equal to 2.2, 4.6 and 5.8 which corresponded to hkl reflection planes 100, 110 and 200, respectively. This means that the synthesized sample has a hexagonal and regular array [27].

The morphology, shape, and approximate particle size of MCM-41 sample were characterized by scanning electron microscope. As can be seen in Figures 2a and b, the synthesized MCM-41 sample has a narrow particle size distribution and uniformly spherical particles. Also, it can be said that the particle size of sample is approximately less than 1000 nanometers. Figure 3 presents transmission electron micrographs of the synthesized MCM-41. The internal morphology observed in Figure 3 shows an uniform pore size on the sample.

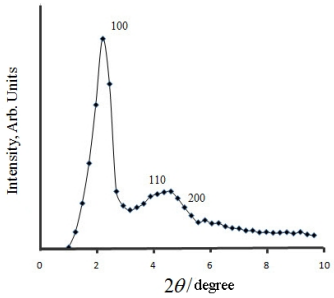


**Figure 1**. XRD pattern of synthesized MCM-41 particles.

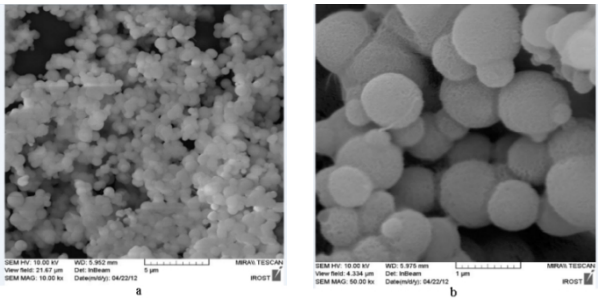

**Figure 2**. SEM micrographs of synthesized MCM-41 particles: (a) 10.00 kx, (b) 50.00 kx.

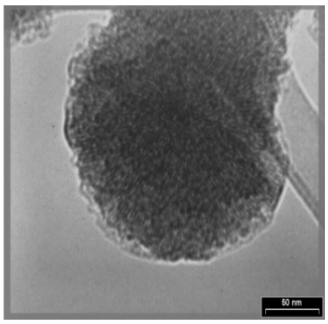

**Figure 3**.TEM view of synthesized MCM-41 particles.

Figure 4a illustrates nitrogen adsorption-desorption isotherm of the synthesized MCM-41, sample S. It can be seen that the sample behaves as mesoporous material during nitrogen adsorption-desorption experiment. The aforementioned behavior is according to IUPAC categorization [28]. A linear increment in nitrogen adsorption takes place at relatively low relative pressures due to monolayer adsorption before the steep nitrogen uptake inside the mesopores. Accordingly, there is micropore filling at low relative pressure. Afterward, at higher pressures an extended multilayer zone and a sharp pore condensation stage can be observed. The steep gas uptake is due to the capillary condensation of nitrogen inside the mesopores. This implies that the synthesized MCM-41 has a narrow pore size distribution. This matter is consistent with the results obtained from XRD experiment. The adsorption and desorption curve demonstrates an obvious loop (type H1 by IUPAC categorization) corresponding to capillary condensation and evaporation on open cylindrical pores at each ends. Furthermore, the higher relative pressure for the capillary condensation is associated with the larger pore size [29].Tzong-Horng Liou[4] synthesized MCM-41 materials by means of the resin waste at varied hydrothermal operation times and temperatures, molar ratios of water to surface agents (CTAB), gelation pH, and drying temperatures.

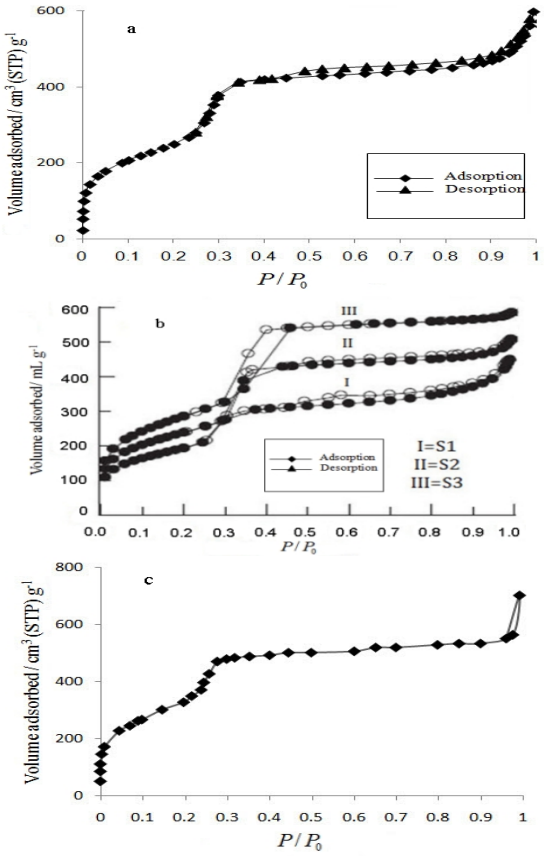


**Figure 4**.Nitrogen adsorption-desorption isotherms: (a) the synthesized MCM-41, (b) the data reported by Tzong-Horng Liou [4], and (c) the data reported by Favas et al.[6].

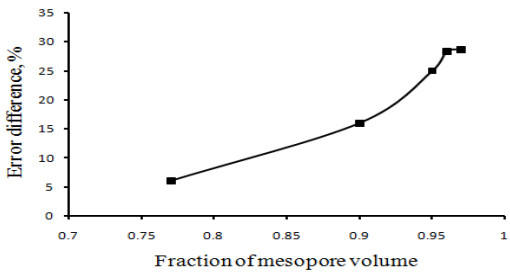


**Figure 5**. Change trend of the error difference Δ versus the fraction of mesopore volume.

**TABLE 1.** Structural parameters of the MCM-41 samples under study

| Sample | $S_{BET}$ ($m^2 g^{-1}$) | $V^a_{total}$ ($cm^3 g^{-1}$) | $V_p$ ($cm^3 g^{-1}$) | $D_p$[d] / Å | $d_{100}$ / Å | $a_0$ / Å | Reference Number |
|---|---|---|---|---|---|---|---|
| **S** | 1163 | 0.903 | 0.814[b] | 30.9 | 40.1 | 46.3 | **Present work** |
| **S1** | 696 | 0.649 | 0.617[b] | 37.3 | 37.9 | 43.8 | [4] |
| **S2** | 860 | 0.744 | 0.717[b] | 34.4 | 38.4 | 44.3 | [4] |
| **S3** | 1033 | 0.887 | 0.859[b] | 34.0 | 37.5 | 43.3 | [4] |
| **S4** | 1205 | 0.981 | 0.754[c] | 32.5 | 35.8 | 41.4 | [6] |

Abbreviations: $S_{BET}$, BET specific surface area; $V_{total}$, total pore volume; $V_p$, mesopore volume; $D_p$, mean pore diameter; $d_{100}$, interplanar distance; $a_0$, lattice parameter.
[a] Adsorbed nitrogen at a relative pressure ($P / P_0$) of approximately 0.99.
[b] Value assessed by BJH method.
[c] Value assessed by $\alpha_s$ plot [32].
[d] Value assessed using $4V_{total} / S_{BET}$.

Figure 4b illustrates nitrogen adsorption-desorption curves of the synthesized MCM-41, samples S1, S2 and S3, that prepared at inert, pH = 9 and pH = 11, conditions, respectively, by Tzong-Horng Liou. It is obvious that these adsorption behaviors are also similar to type IV isotherm according to IUPAC categorization. There is a loop in all three curves. However, the loop corresponding to S3 sample is wider than other two samples. That means that there is larger mesopores in S3 sample than that of in both of samples S1 and S2.

Also, adsorption capacity increases with an increment in pH showing an increase in pore volume. Figure 4c illustrates nitrogen adsorption-desorption data of a synthesized MCM-41 by Favas et al.[6]. this adsorption manner is similar to four previous samples, S, S1, S2 and S3. However, there is a difference in relation to hysteresis loop between this sample, S4, and four previous samples. It can be seen in Figure 4c that there isn't any loop in nitrogen adsorption-desorption curve of sample S4. The absence of a loop for such materials is attributed to the pore size, which lies between the micropore and mesopore regions [30, 31].

Table 1 lists the textural properties and the XRD data of samples S, S1, S2, S3 and S4. As can be seen in Table 1, the properties of the synthesized MCM-41, sample S, are very close to other samples. However, the BET surface area of the sample S is higher than samples S1, S2 and S3. Also, the mean pore size, $D_p$, of sample S is the lowest among the other samples. The interplanar distance, $d_{100}$, and the lattice parameter, $\alpha$ , also were calculated and reported in Table 1.

4. 2. Analysis of Theoretical Approach As mentioned earlier, the DA equation (Equation (1)) is valid over a range of $N_2$ relative partial pressure $P/P_0$ varying from 1E-7 to 0.02, and the DR equation (Equation (2)) is valid over two ranges of $N_2$ relative partial pressure $P/P_0$ varying from 1E-7 to 0.02 and 0.01 to 0.1. Thus, the adsorption isotherms were fitted to the DA and DR equations over ranges of $N_2$ relative partial pressure varying from 1E-7 to 0.02 and 0.01 to 0.1, respectively. Table 2 presents the obtained results, the micropore volume $w_0$, from fitting the adsorption isotherms of samples S, S1, S2, S3 and S4 to both the DA and DR equations. With attention to the correlation coefficients, $R^2$, it can be deduced that the adsorption isotherms have properly correlated to the both isotherm models.

**TABLE 2.** DA and DR's $w_0$ of the MCM-41 samples under study

| Sample | $w_0^{DA}$ $cm^3 g^{-1}$ | $w_0^{DR}$ $cm^3 g^{-1}$ | $R^2_{DA}$ | $R^2_{DR}$ |
|---|---|---|---|---|
| **S** | 0.162 | 0.226 | 0.981 | 0.983 |
| **S1** | - | 0.192 | - | 0.986 |
| **S2** | - | 0.231 | - | 0.967 |
| **S3** | - | 0.275 | - | 0.987 |
| **S4** | 0.198 | 0.277 | 0.987 | 0.972 |

Abbreviations: $w_0^{DA}$, the micropore volume calculated using DA equation; $w_0^{DR}$, the micropore volume calculated using DR equation; $R^2_{DA}$, Correlation coefficient in fitting the isotherm data to DA equation; $R^2_{DR}$, Correlation coefficient in fitting the isotherm data to DR equation.

**TABLE 3.** Mesopore volume of MCM-41samples under study

| Sample | $V_P$ $cm^3 g^{-1}$ | $V_{P1}$ $cm^3 g^{-1}$ | $V_{P2}$ | $V_P / V_{total}$ | $\Delta^a_{P1}$ | $\Delta^a_{P2}$ |
|---|---|---|---|---|---|---|
| **S** | 0.814 | 0.741 | 0.677 | 0.9 | 8 | 16 |
| **S1** | 0.617 | - | 0.457 | 0.95 | - | 25 |
| **S2** | 0.717 | - | 0.513 | 0.96 | - | 28.4 |
| **S3** | 0.859 | - | 0.612 | 0.97 | - | 28.7 |
| **S4** | 0.754 | 0.783 | 0.704 | 0.77 | 3 | 6 |

Abbreviations: $V_{P1}$, the mesopore volume obtained by subtracting $V_{total}$ from $w_0^{DA}$, $V_{P2}$, the mesopore volume obtained by subtracting $V_{total}$ from $w_0^{DR}$.
[a] $\Delta_X$ is the error difference: $\Delta_X\% = \frac{V_P - V_X}{V_P} \times 100$ .

.

**TABLE 4.** Pore size of MCM-41 samples under study

| Sample | $D_p$ (Å) | $D_m$ (Å) | $D^c_{XRD}$ (Å) | $D^{DA}_{Eq.7}$ (Å) | $D^{DR}_{Eq.7}$ Å | $\Delta^{DA,d}_{Eq.7}$ | $\Delta^{DR,d}_{Eq.7}$ | $\Delta^{DA,e}_{Eq.7}$ | $\Delta^{DR,e}_{Eq.7}$ |
|---|---|---|---|---|---|---|---|---|---|
| S | 30.9 | 34.6[a] | 38.6 | 37.9 | 37.2 | 1 | 3 | 8 | 6 |
| S1 | 37.3 | - | 34.5 | - | 32.1 | - | 7 | - | - |
| S2 | 34.4 | - | 36.0 | - | 33.5 | - | 7 | - | - |
| S2 | 34.0 | - | 36.4 | - | 34.0 | - | 6 | - | - |
| S4 | 32.5 | 34.2[b] | 34.1 | 34.4 | 33.7 | 0 | 1 | 0 | 1 |

Abbreviations: $D_m$, the pore diameter; $D^{DA}_{Eq.7}$, the pore diameter calculated by Equation( 7) and $w_0^{DA}$ value,$D^{DR}_{Eq.7}$, the pore diameter calculated by Equation (7) and $w_0^{DR}$ value.

[a] Value assessed using BJH method.

[b] Value assessed using NLDFT method [6, 33, 34].

[c] Values calculated by Equation (4).

[d] $\Delta^y_X$ is the error difference: $\Delta^y_X\% = \frac{D_{XRD} - D^y_X}{D_{XRD}} \times 100$ .

[e] $\Delta^y_X$ is the error difference: $\Delta^y_X\% = \frac{D_m - D^y_X}{D_m} \times 100$ .

In this study, the mesopore volume of samples were calculated by subtracting $V_{total}$ from $w_0$ and compared with the obtained mesopore volume using other methods. Table 3 summarizes the results. As can be seen in Table 3, with increasing the fraction of mesopore volume, $V_P/V_{total}$, the error difference $\Delta$ is increased (Figure 5).Additionally, on samples S1, S2 and S3, with the fraction of mesopore volume > 0.9, the error difference $\Delta$ is higher than 20%. Likewise, the lowest error difference $\Delta$, around 5%, is observed on sample S4, its fraction of mesopore volume is equal to 0.77. Finally, it can be said that on the samples with the fraction of mesopore volume $\leq$ 0.9 the calculated mesopore volumes had good consistency with the obtained mesopore volumes by other methods.

Also, with attention to the obtained result on samples S and S4, $\Delta P_1$and $\Delta P_2$, it can be said that the obtained mesopore volume using DA model, $V_{P1}$, is more consistent than the calculated mesopore volume by DR model, $V_{P2}$, to the obtained mesopore volume using BJH and $\alpha_s$ plot methods.

The Equations (4) and (7) were applied to calculate the pore diameter of samples. In fact, the mentioned calculations were performed to examine that whether the obtained pore diameter of samples using Equation (7) would be consistent to the calculated pore diameter of samples by Equation (4) and also to the obtained results using other methods

It must be mentioned that in Equation (4) was used $V_p$ values as mesopore volume (see Table 1). Table 4 shows the results. As can be seen in Table 4, in all samples, the pore diameters calculated by Equation (7) have good consistency, $\Delta^{DA,d}_{Eq.7}$ and $\Delta^{DR,d}_{Eq.7}$, to the obtained pore diameter using Equation (4). Moreover, the consistency on samples S and S4, with the fraction of mesopore volume $\leq$ 0.9, is better than that of other samples, with the fraction of mesopore volume > 0.9.

Likewise, the calculated pore diameters of samples S and S4 using Equation (7) are very close, $\Delta^{DA,e}_{Eq.7}$ and $\Delta^{DR,e}_{Eq.7}$, to the obtained pore diameter of the samples by BJH and NLDFT methods, respectively. However, these consistencies on sample S4 are further, the error differences $\Delta$ are lower, than sample S.

## 5. CONCLUDING REMARKS

Evaluation of mesoporosity and pore size of MCM-41 particles by an accurate method is very important. BJH method are very often used for the purpose. The method is somewhat complicated and time consuming. Therfore, using a simpler and faster method instead of BJH is very useful. DA and DR equations can be used to calculate the mesoporosity of the MCM-41 samples. The procedure are swift and neat. However, accuracy of the methods to assess mesopore volume and pore size of the MCM-41 particles have not been studied yet. In this study, the mesopore volume and pore size of several MCM-41 samples were calculated using Dubinin-Astakhov and Dubinin-Radushkevic isotherm models and by utilizing nitrogen adsorption isotherms and XRD data. The obtained results also compared with the mesopore volume and pore size calculated by other methods. It was concluded when fraction of mesopore volume is higher than 0.9 the calculated mesopore volume and pore size of the samples were in good consistency with XRD data and other advanced simulation techniques.

## 6. REFERENCE

1. Anbia, M. and Ghaffari, A., "Modified nanoporous carbon material for anionic dye removal from aqueous solution", ***International Journal of Engineering-Transactions B: Applications***, Vol. 25, No. 4, (2012), 259.

2. Anbia, M., and Davijani, H.A. and "Preparation and structural characterization of a novel nanoporous carbon (cmk-3) functionalized with ethylenediamine its use in removal of cu(ii)

and pb(ii) ions from aqueous media", ***International Journal of Engineering-Transactions B: Applications***, Vol. 27, (2014), 1425-1434.

3. Ghorbani, F., Younesi, H., Mehraban, Z., Celik, M.S., Ghoreyshi, A. and Anbia, M., "Aqueous cadmium ions removal by adsorption on aptms grafted mesoporous silica mcm-41 in batch and fixed bed column processes", ***International Journal of EngineeringTransaction B: Applications***, Vol. 26, No. 5, (2013).
4. Liou, T.-H., "A green route to preparation of mcm-41 silicas with well-ordered mesostructure controlled in acidic and alkaline environments", ***Chemical Engineering Journal***, Vol. 171, No. 3, (2011), 1458-1468.
5. Ravikovitch, P.I. and Neimark, A.V., "Characterization of nanoporous materials from adsorption and desorption isotherms", ***Colloids and Surfaces A: Physicochemical and Engineering Aspects***, Vol. 187, (2001), 11-21.
6. Favvas, E.P., Mitropoulos, A.C. and and Stefanopoulos, K.L., "Simple equation for accurate mesopore size calculations", ***Micropore and Mesopore Material***, Vol. 145, (2011), 9-13.
7. Zhai, S.R., Wei, Z.P., An, Q.D., Wub, D. and Sun, Y.H., "Facile assembly of dispersed zrmcm-41 nanoparticles promoted in-situ by zirconium salt", ***Journal of the Chinese Chemical Society***, Vol. 58, No. 2, (2011), 181-185.
8. Emine, K., Nuray O., K., G., and Kırali, M. and "Synthesis and characterization of ba/mcm-41", ***Turkish Journal of Chemistry***, Vol. 34, (2010), 935-943.
9. Freundlich, H. and Hatfield, H.S., "Colloid and capillary chemistry", (1926).
10. Langmuir, I., "The adsorption of gases on plane surfaces of glass, mica and platinum", ***Journal of the American Chemical society***, Vol. 40, No. 9, (1918), 1361-1403.
11. Zeldowitsh, J., " Acta phisicochimica urss", Vol. 1, (1935).
12. Brunauer, S., Emmett, P.H. and Teller, E., "Adsorption of gases in multimolecular layers", ***Journal of the American Chemical society***, Vol. 60, No. 2, (1938), 309-319.
13. Terzyk, A.P., Gauden, P.A. and Kowalczyk, P., "What kind of pore size distribution is assumed in the dubinin–astakhov adsorption isotherm equation?", ***Carbon***, Vol. 40, No. 15, (2002), 2879-2886.
14. Dubinin, M.M., Gregg, S.J., Sing, K.S.W. and and Stoeckli, H.F., "Characterisation of porous solids", ***London, England, The Society of Chemical Industry***, (1979).
15. Dubinin, M. and Radushkevich, L., "Equation of the characteristic curve of activated charcoal", ***Chem. Zentr***, Vol. 1, No. 1, (1947), 875-884.
16. Carvalho, A., Mestre, A., Pires, J., Pinto, M. and Rosa, M.E., "Granular activated carbons from powdered samples using clays as binders for the adsorption of organic vapours", ***Microporous and Mesoporous Materials***, Vol. 93, No. 1, (2006), 226-231.
17. Gaspard, S., Altenor, S., Dawson, E.A., Barnes, P.A. and Ouensanga, A., "Activated carbon from vetiver roots: Gas and liquid adsorption studies", ***Journal of Hazardous Materials***, Vol. 144, No. 1, (2007), 73-81.
18. Olivares-Marín, M., Fernández-González, C., Macías-García, A. and Gómez-Serrano, V., "Preparation of activated carbon from cherry stones by chemical activation with zncl< sub> 2</sub>", ***Applied Surface Science***, Vol. 252, No. 17, (2006), 5967-5971.
19. Barrett, E.P., Joyner, L.G. and Halenda, P.P., "The determination of pore volume and area distributions in porous substances. I. Computations from nitrogen isotherms", ***Journal of the American Chemical Society***, Vol. 73, No. 1, (1951), 373-380.
20. Grün, M., Unger, K.K., Matsumoto, A. and Tsutsumi, K., "Novel pathways for the preparation of mesoporous mcm-41 materials: Control of porosity and morphology", ***Microporous and Mesoporous Materials***, Vol. 27, No. 2, (1999), 207-216.
21. Ciesla, U. and Schüth, F., "Ordered mesoporous materials", ***Microporous and Mesoporous Materials***, Vol. 27, No. 2, (1999), 131-149.
22. Kruk, M., Jaroniec, M. and Sayari, A., "Adsorption study of surface and structural properties of mcm-41 materials of different pore sizes", ***The Journal of Physical Chemistry B***, Vol. 101, No. 4, (1997), 583-589.
23. Jaroniec, M. and Solovyov, L.A., "Assessment of ordered and complementary pore volumes in polymer-templated mesoporous silicas and organosilicas", ***Chem. Commun.***, No. 21, (2006), 2242-2244.
24. Kim, B.-J., Bae, K.-M. and Park, S.-J., "A study of the optimum pore structure for mercury vapor adsorption", ***Bulletin of the Korean Chemical Society***, Vol. 32, No. 5, (2011), 1507-1510.
25. Jomekian, A., Pakizeh, M., Shafiee, A.R. and Mansoori, S.A.A., "Fabrication or preparation and characterization of new modified mcm-41/psf nanocomposite membrane coated by pdms", ***Separation and Purification Technology***, Vol. 80, No. 3, (2011), 556-565.
26. Chen, H. and and Wang, Y.C., ***Cermics Inernational*** Vol. 28, (2002), 541.
27. Lin, H.P., Tang, C.Y. and Lin, C.Y., "Detailed structural characterizations of sba-15 and mcm-41 mesoporous silicas on a high-resolution transmission electron microscope", ***Journal of the Chinese Chemical Society***, Vol. 49, No. 6, (2002), 981-988.
28. Sing, K.S., "Reporting physisorption data for gas/solid systems with special reference to the determination of surface area and porosity (recommendations 1984)", ***Pure and applied chemistry***, Vol. 57, No. 4, (1985), 603-619.
29. Mitropoulos, A.C. and "Capillarity", ***Journal of Engineering Science and Technology Review***, Vol. 2, (2009), 28.
30. Inoue, S., Hanzawa, Y. and Kaneko, K., "Prediction of hysteresis disappearance in the adsorption isotherm of n2 on regular mesoporous silica", ***Langmuir***, Vol. 14, No. 11, (1998), 3079-3081.
31. Neimark, A.V., Ravikovitch, P.I. and Vishnyakov, A., "Adsorption hysteresis in nanopores", ***Physical Review E***, Vol. 62, No. 2, (2000), R1493.
32. Gregg, S. and Sing, K.S., "Adsorption, surface area, and porosity", (1983).
33. Tarazona, P., "Free-energy density functional for hard spheres", ***Physical Review A***, Vol. 31, No. 4, (1985), 2672.
34. Klomkliang, N., Do, D. and Nicholson, D., "On the hysteresis and equilibrium phase transition of argon and benzene adsorption in finite slit pores: Monte carlo vs.Bin-Monte Carlo", ***Chemical Engineering Science***, Vol. 87, (2013), 327-337.

# Studying Performance of Dubinin-astakhov and Dubinin-raduchkevic Equations to Evaluate Nanopore Volume and Pore Size of MCM-41 Particles

N. Saeidi, M. Parvini, M. R. Sarsabili

*School of Chemical, Gas and Petroleum Engineering, Semnan University, Semnan, Iran*

*PAPER INFO*

*Paper history*:
Received 15 February 2014
Received inrevised form 18 June 2014
Accepted 26 June 2014

*Keywords*:
Nitrogen Isotherm Data,
MCM-41
Dubinin-astakhov and Dubinin-Raduchkevic Equations
Nanopore (Mesopore) Volume
Pore Size

**چکیده**

ذرات ام سی ام 41 با استفاده از مواد خام غیر آلی و ستیل تری متیلامونیوم برمید سنتز شد. خصوصیات ساختاری و بافتی اش به وسیله تست های ایکس آر دی، اس ای ام، تی ای ام و جذب- دفع هم دمای نیتروژن بررسی شد. برای بررسی کارایی معادلات هم دمای دوبینین آستاخوف و دوبینین راداچکویچ در ارزیابی کردن حجم مزو حفرات و اندازه حفرات نمونه های ام سی ام 41، حجم مزو حفرات و اندازه حفرات چندین نمونه از ذرات ام سی ام 41 به وسیله دو مدل هم دمای ذکر شده و با استفاده از داده های به دست آمده از جذب- دفع هم دمای نیتروژن و ایکس آر دی، محاسبه شد. نتایج به دست آمده در مورد حجم مزو حفرات و اندازه حفرات محاسبه شده با دو مدل ذکر شده، با حجم مزو حفرات و اندازه حفرات محاسبه شده با دیگر روش های پیشرفته مقایسه شد. نتایج نشان دادند که حجم مزو حفرات و اندازه ذرات محاسبه شده با دو مدل ذکر شده در مورد نمونه هایی که کسر حجم مزو حفرات شان از 0/9 بیشتر است سازگاری مناسبی با داده های به دست آمده از ایکس آر دی و روش های دیگر، ندارند. هرچند، حجم مزو حفرات و اندازه حفرات محاسبه شده با دو روش هم دمای ذکر شده و در مورد نمونه هایی که کسر حجم مزو حفرات شان کم تر از 0/9 است سازگاری مناسبی با داده های به دست آمده از ایکس آر دی و دیگر تکنیک های شبیه سازی پیشرفته، دارند.

*doi: 10.5829/idosi.ije.2014.27.10a.04*